

# Supporting Information

## Light-Stimulated Permanent Shape Reconfiguration in Crosslinked Polymer Microparticles

*Lewis Michael Cox,<sup>1, 2, 5, \*</sup> Xiaohao Sun,<sup>1, 3</sup> Chen Wang,<sup>2</sup> Nancy Sowan,<sup>2, 4</sup> Jason P. Killgore,<sup>5</sup>  
Rong Long,<sup>1</sup> Heng-An Wu,<sup>3</sup> Christopher N. Bowman,<sup>2, 4</sup> and Yifu Ding<sup>1, 4, \*</sup>*

<sup>1</sup> Department of Mechanical Engineering, University of Colorado, Boulder, CO 80309-0427,  
USA

<sup>2</sup> Department of Chemical and Biological Engineering, University of Colorado, Boulder, CO  
80309-0596, USA

<sup>3</sup> CAS Key Laboratory of Mechanical Behavior and Design of Materials, Department of Modern  
Mechanics, University of Science and Technology of China, Hefei, Anhui 230027, China

<sup>4</sup> Material Science and Engineering Program, University of Colorado, Boulder, CO 80309-0596,  
USA

<sup>5</sup> Applied Chemicals and Materials Division, National Institute of Standards and Technology,  
Boulder, CO 80305, USA

\*Email: lewis.cox@nist.gov and yifu.ding@colorado.edu

## 1. Particle Size Distribution

The diameter of as-synthesized, unswollen CANs particles was  $3.1 \mu\text{m} \pm 0.3 \mu\text{m}$  (average  $\pm$  standard deviation,  $N = 30$ ), according to atomic force microscopy (AFM) measurements. A histogram showing particle size distribution is presented in Fig. S1.

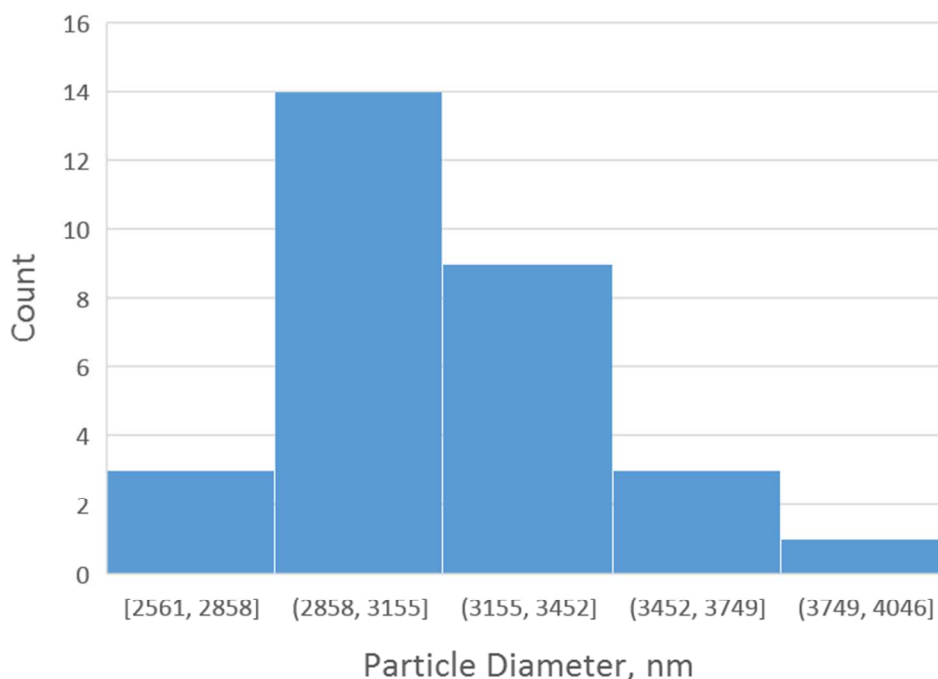


**Figure S1.** Results from AFM scans illustrate the distribution of particle size resulting from the dispersion polymerization process.

## 2. Fitting AFM Force-Displacement Curves

Different contact models were fit to the experimental force displacement curves in order to calculate the modulus of the particles (Fig. S2): Hertzian, Johnson-Kendall-Roberts (JKR), and Derjaguin-Muller-Toporov (DMT). As expected for compliant spheres the JKR model showed the closest fit to the data. A total of 5 particles were examined with 16 curves performed on each particle surface. The final calculated particle modulus was found to be  $12 \text{ MPa} \pm 1 \text{ MPa}$ .

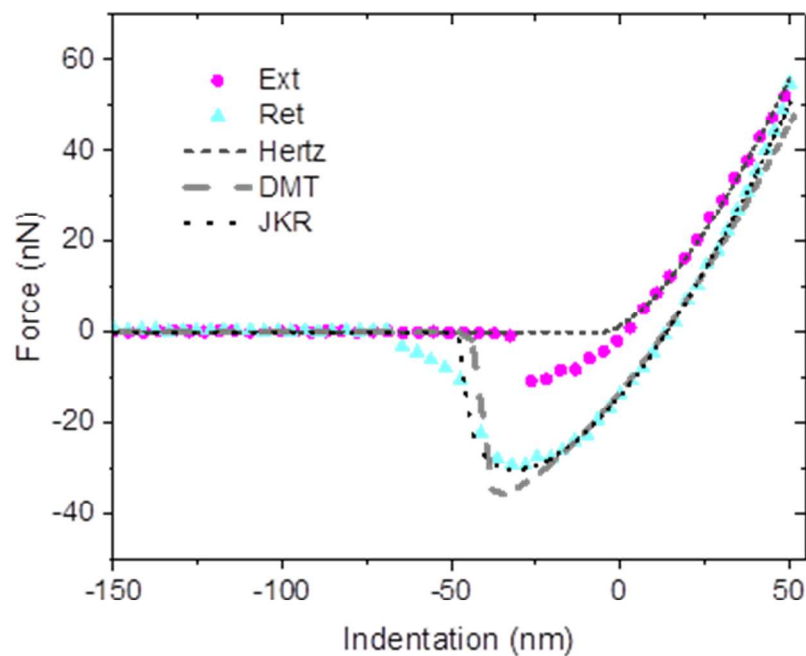


**Figure S2.** AFM probe is extended (Ext) until it pushes into a particle, it is then retracted (Ret). Multiple contact models are fit to the force displacement data with JKR generating the best representation.

### 3. Dynamic Mechanical Analysis (DMA)

DMA measurements were taken from -50 °C to 30 °C at a rate of 3 °C/min, under a strain amplitude of 0.1 %. The glass transition temperature ( $T_g$ ) is located at the  $\tan \delta$  peak and is determined from Fig. S3 to be -15 °C.

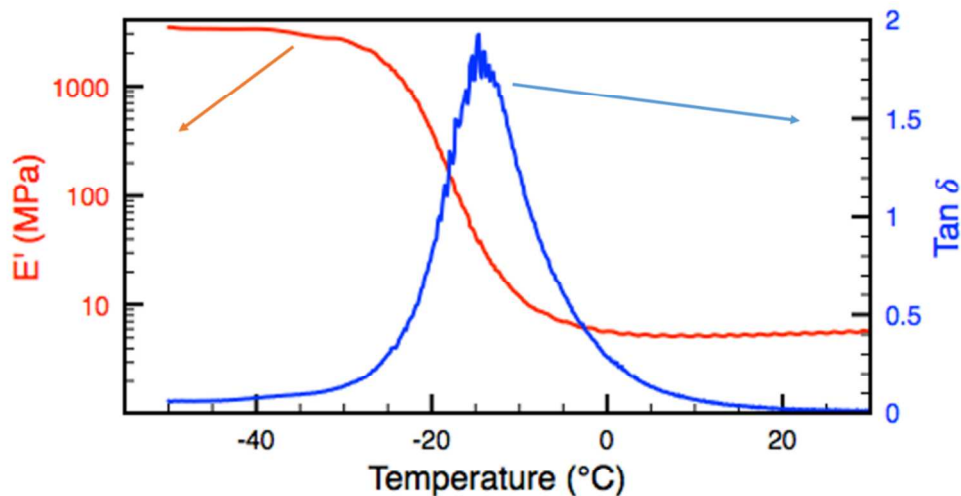


**Figure S3.** DMA temperature scan of a film with similar chemistry to that of the RAFT particles.

#### 4. Finite Element Simulation

Finite element model (FEM) simulations of the partial recovery of RAFT particles were performed using a commercial software ABAQUS (v6.14, Dassault Systemes Simulia Corp., Providence, RI). The FEM consists of a spherical RAFT particle with radius of  $R$  between two parallel rigid plates. The radius  $R$  is scaled according to the actual particle radius measured by AFM. Axisymmetry allows us to capture the three-dimensional particle deformation using a two-dimensional axisymmetric model consisting of a cross-section of the particle and the rigid plates. The model geometry is meshed with the 4-node bilinear hybrid axisymmetric elements (CAX4H). The particles are compressed by the rigid plates to simulate the process of nanoimprint lithography (NIL) applied in experiments. The loading process consists of three steps:

*Step 1: Mechanical loading.* A prescribed compression is applied to the particle by moving down the top plate while fixing the bottom plate. The top plate is compressed down until a final spacing  $s$  is reached between the two rigid plates. An average compressive strain can then be calculated as  $(d-s)/d$ , where  $d = 2R$  is the particle diameter. In this step, the neo-Hookean model is employed to simulate the elastic deformation of the particle, and we assumed frictionless contact between the particle and the two plates.

*Step 2: UV exposure / stress relaxation.* This step is to simulate the effect of UV irradiation under fixed compression in the experiment. Our The UV light activated RAFT in polymer network, which causes network rearrangement and stress relaxation within the particle. Our FE model is capable of simulating such stress relaxation. Specifically, the Cauchy stress is relaxed to  $s_t = fs_0$ , where  $s_0$  is the Cauchy stress in the deformed particle at the end of Step 1. The parameter  $f$  denotes the stress relaxation ratio and is set to be uniform within the particle. This is based on the assumption that the UV light intensity is uniform within the compressed particle, i.e. we neglected any light attenuation effect due to the small spacing,  $s$  ( $\sim \mu\text{m}$ ). The stress relaxation behavior is not readily available in the built-in material library of ABAQUS, and is captured in our simulation by a customized material model through a user subroutine (UMAT).

*Step 3: Release.* When stress relaxation is completed, the applied deformation is released, and a permanent non-spherical particle will be achieved. The new shape depends on the extent of stress relaxation during Step 2 and is the main result of the FE simulation. In this step, the stress relaxation is turned off since there is no UV irradiation.

## 5. Scanning Electron Microscopy of CAN Particles

All imaging was done using a 5 kV voltage and a 10  $\mu$ A filament current. Fig. S4a&b present top-down images of a single particle before and after focusing the electron beam onto its surface. Images indicate that large deformations occur while focusing on the particle. For top-down images, the ability to focus on the nearby substrate, rather than on the particle itself, allows for easy imaging of the particle geometry. In Fig. 2b, from the main body of the text, the 90 ° SEM images require long focus times directly on the particle. The highly wrinkled morphologies in the images are due to the SEM itself and do not provide a true depiction of the geometries achieved during the NIL process.

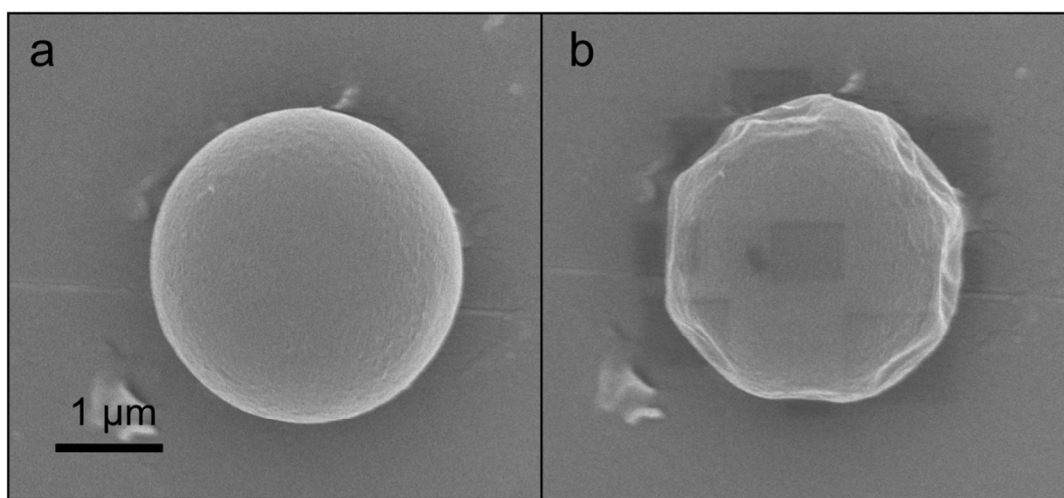


**Figure S4.** a) An as-cast particle is imaged by focusing on the nearby substrate, b) the same particle is then imaged after repeatedly focusing the electron beam on different domains of the particle surface, inducing large deformations.

## 6. Local Shape Reconfiguration on CAN Particle Surfaces with AFM

Fig. S5 shows representative surface coverage of particles on the substrate. To generate indentations on a particle surface, the AFM tip is pushed into the particle surface and exposed to the blue-drive LED, Fig S5. The resulting particle geometry is shown in Fig. S6.

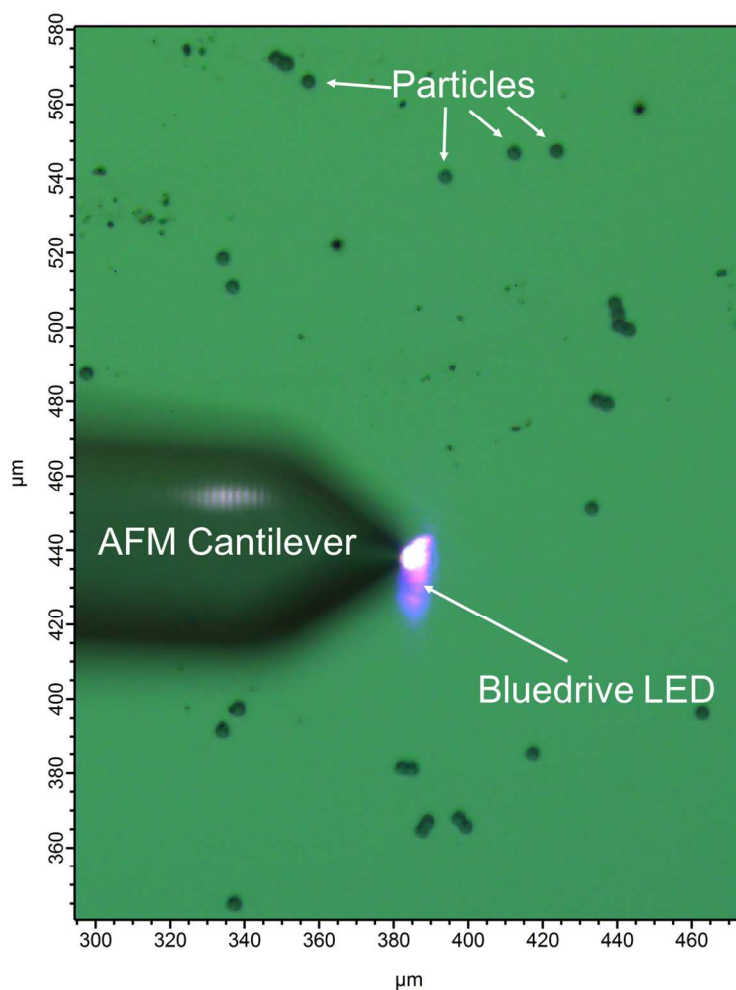


**Figure S5.** Optical microscope image of particles dispersed onto an  $\text{SiO}_x$  substrate. The AFM probe tip (not visible) protrudes out from the right of the AFM cantilever and down towards the substrate. The Blue-drive LED is positioned directly over the AFM tip.

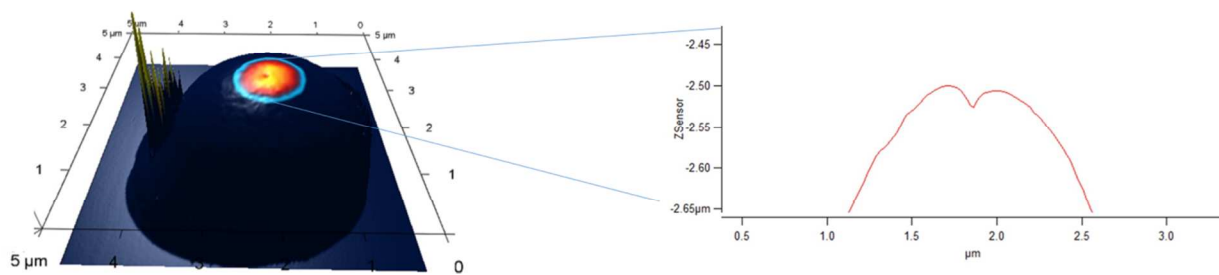


**Figure S6.** Full AFM scan of particle shown in Fig. 3C after indentation using AFM tip (left). Cross section of the indentation (right).